Received: 15 January 2018 | Revised: 22 May 2018 | Accepted: 9 June 2018

DOI: 10.1002/ett.3475

RESEARCH ARTICLE

WILEY

Error performance of power line communications in the presence of Nakagami-*m* background noise

Vasilis K. Papanikolaou[1] | Georgia D. Ntouni[1] | Alexandros-Apostolos A. Boulogeorgos[1,2] | George K. Karagiannidis[1]

[1]Department of Electrical and Computer Engineering, Aristotle University of Thessaloniki, Thessaloniki, Greece

[2]Department of Digital Systems, University of Piraeus, Piraeus, Greece

Correspondence
George K. Karagiannidis, Department of Electrical and Computer Engineering, Aristotle University of Thessaloniki, 54636 Thessaloniki, Greece.
Email: geokarag@auth.gr

Funding information
Alexander Onassis Foundation

Abstract

This paper studies the error performance of power line communication (PLC) systems, in the presence of background noise with Nakagami-*m* distributed envelope and uniformly distributed phase. In this sense, we present closed-form expressions for the symbol error rate (SER) of PLC systems using binary pulse amplitude modulation and generalize the analysis to accommodate the *M*-ary pulse amplitude modulation. In addition, novel closed-form expressions for the SER upper bound of rectangular quadrature amplitude modulation PLC systems are derived. Interestingly, these expressions can be considered as tight SER approximations in the high–signal-to-noise ratio region and, thus, can efficiently evaluate the operational bound of a PLC system.

1 | INTRODUCTION

In recent years, the concept of power line communication (PLC) has emerged, owing to the need to provide high-data-rate, reliable, and low-cost access for indoor and outdoor applications.[1] Taking advantage of the ubiquitous presence of power cables, PLC provides a feasible solution for several applications, such as smart grid[2] and in-home networking (eg, HomePlug AV).[3] Interestingly, the main challenge in PLC lies in the particularities of the transmission medium, which results in high cable attenuation, frequency selectivity, and non-Gaussian noise. Particularly, although communication signals are transmitted at high frequencies (ie, in the MHz band), power cables are designed to transfer low-frequency power signals. To this end, a great amount of effort has been put on analyzing the performance of PLC systems[4-16] as well as on presenting new transmission and reception schemes.[17,18]

In general, the additive channel noise in PLC is classified into two categories: the *background noise* and the *impulsive noise*.[4,16] The impulsive noise is of short duration, has a high power spectral density, and is commonly represented by a Poisson or Middleton Class A distribution. Ndo et al[15] quantified the performance of PLC systems assuming only impulsive noise. However, in this paper, we only study the effect of background noise, which is the dominant one in PLC systems, as the impulsive noise occurs randomly and has been proven to be efficiently reduced by the use of proper channel coding.[10]

The background noise includes both colored and narrowband components. Despite the paramount impact of noise in the performance of PLC systems, its non-Gaussian nature has been overlooked in several studies, where, for the sake of simplicity, the background noise has been described as an additive white Gaussian process.[18] Interestingly, experimental results have revealed that the envelope of the background noise follows a Nakagami-*m* distribution.[4] Due to the fact that Nakagami-*m* contains the half Gaussian, the Rayleigh, and the Gaussian distribution as special cases, it has been proven to be a robust and general model for the description of the noise particularities in PLC systems.

The impact of Nakagami-*m* background noise on the performance of a PLC system in terms of the error rate and outage probability has been studied in the literature.[5-14] Particularly, Kim et al[6] presented a closed-form expression for the

probability distribution function (PDF) of the Nakagami-m noise, whereas expressions for the bit error rate of PLC systems using binary phase-shift keying (BPSK) and quadrature phase-shift keying (QPSK) modulation, respectively, were proposed in more recent works.[7,8] However, we highlight that the presented expressions are not in closed form. Moreover, Chattopadhyay et al[9] and Mathur et al[10,11,13] studied PLC systems under Nakagami-m noise considering binary frequency-shift keying, BPSK, differential BPSK, and QPSK, while also providing the optimum detection conditions. Finally, Dash et al presented a diversity scheme for PLC systems operating in Nakagami-m noise environments.[17]

In the literature, the effect of Nakagami-m background noise on the PLC systems' performance has been investigated, assuming modulations with one degree of freedom or QPSK. However, in practice, PLC systems use modulation schemes with two degrees of freedom,[7,8,11] such as quadrature amplitude modulation (QAM), whose error performance has not been addressed yet. The technical contributions of this paper are outlined below.

- We first derive novel closed-form expressions for the symbol error rate (SER) of PLC systems using binary pulse amplitude modulation (BPAM) in the presence of Nakagami-m background noise.
- Next, we generalize the analysis in order to accommodate the M-ary pulse amplitude modulation (PAM) case.
- Utilizing the derived SER for the M-PAM, we provide the mathematical framework to evaluate and quantify the error performance of PLC systems in the presence of Nakagami-m background noise using rectangular QAM (RQAM). More precisely, we derive novel closed-form expressions for the upper bound of the SER corresponding to this PLC system.
- Low-complexity expressions, which provide useful technical insights, are derived for the special case of $m = 0.5$.
- Finally, respective simulation results are presented to validate the proposed mathematical framework.

This paper is organized as follows. Section 2 includes the system model of our analysis, whereas in Section 3, we provide the error performance analysis under the assumption of BPAM, M-PAM, and RQAM. Respective numerical results and discussions are presented in Section 4, and finally, we conclude with closing remarks in Section 5.

Notation: In the sequel, $|x|$ stands for the absolute value or modulus or magnitude of a complex number x, whereas $\Gamma(\cdot)$ and $\exp(\cdot)$ stand for the Gamma function (see equation (8.310) in the work of Gradshteyn and Ryzhik[19]) and the exponential function, respectively. Moreover, $\mathrm{sgn}(\cdot)$ represents the sign or signum function, and $\mathrm{erfc}(\cdot)$ represents the complementary error function. Additionally, ${}_pF_q(\alpha_1, \ldots, \alpha_p; \beta_1, \ldots, \beta_q; \cdot)$ stands for the generalized hypergeometric function,[20] whereas ${}_1F_1(\cdot, \cdot, \cdot)$ stands for the confluent hypergeometric function of the first kind. The zero-order modified Bessel function of the second kind is represented as $K_0(\cdot)$ (see equation (8.407/1) in the work of Gradshteyn and Ryzhik[19]), whereas the Meijer G-function is represented as $G_{p,q}^{k,l}\left(\begin{matrix} \alpha_1, \ldots, \alpha_p \\ \beta_1, \ldots, \beta_q \end{matrix} \middle| \cdot \right)$ (see equation (9.301) in the work of Gradshteyn and Ryzhik[19]). Finally, $\Pr(\mathcal{A})$ stands for the probability of event $\mathcal{A}$, whereas $\Pr(\mathcal{A}|\mathcal{B})$ stands for the probability of $\mathcal{A}$ under the condition that event $\mathcal{B}$ is satisfied.

2 | SYSTEM AND SIGNAL MODEL

In this paper, a point-to-point PLC system affected by background noise, whose envelope follows the Nakagami-m distribution, is considered. More specifically, a signal, s, is transmitted over an additive noise channel, n. The received passband signal passes through various processing stages, also known as the front-end of the receiver, which include filtering, amplification, analog in-phase and quadrature demodulation, down-conversion to baseband, and sampling. Thus, the baseband equivalent of the received signal can be expressed as

$$r = s + n \tag{1}$$

and is forwarded to a maximum likelihood detector, where an estimation $\tilde{s}$ of the transmitted signal is derived.

In order to facilitate the analysis, we write n as

$$n = n_I + j\, q\, n_Q, \tag{2}$$

where n_I and n_Q represent the in-phase and quadrature components of n, respectively, and are equal to

$$n_I = |n| \cos\theta \text{ and } n_Q = |n| \sin\theta. \tag{3}$$

Note that q is a parameter standing for the dimension of the modulation, ie, $q = 0$ indicates that s is a one-dimensional modulated signal, whereas $q = 1$ indicates that s is a two-dimensional modulated signal.

The phase θ of the noise is considered a random variable (RV) with uniform distribution in $(-\pi, \pi]$.[4] Finally, the PDF of the Nakagami-m distributed RV, $|n|$, ie, the envelope of the noise, is equal to[4]

$$f_{|n|}(x) = \frac{2}{\Gamma(m)}\left(\frac{m}{\Omega}\right)^m x^{2m-1}\exp\left(-\frac{mx^2}{\Omega}\right), \tag{4}$$

where m and Ω stand for the shape and spread parameters, respectively.

3 | ERROR PERFORMANCE ANALYSIS

In this section, we present the mathematical framework for the quantification of the impact of Nakagami-m background noise in the error performance of PLC systems evaluated in terms of the SER.

3.1 | Statistical background

For practical PLC applications, it has been experimentally proven[4,5] that $m \in [0.5, 1]$. In this case, according to Kim et al,[6] the PDF of n_I can be evaluated as

$$f_{n_I}(y) = \frac{1}{\Gamma(m)\sqrt{\pi}}\sqrt{\frac{m}{\Omega}}\exp\left(-\frac{my^2}{\Omega}\right)\left\{\frac{\Gamma(0.5-m)}{\Gamma(1-m)}\left(\frac{my^2}{\Omega}\right)^{m-\frac{1}{2}}{}_1F_1\left(\frac{1}{2}, \frac{1}{2}+m, \frac{my^2}{\Omega}\right)\right.$$
$$\left. + \frac{1}{\sqrt{\pi}}\Gamma(m-0.5)\,{}_1F_1\left(1-m, \frac{3}{2}-m, \frac{my^2}{\Omega}\right)\right\}. \tag{5}$$

In the half-Gaussian scenario, ie, $m = 0.5$, this PDF reduces to

$$f_{n_I}(y; m=0.5) = \frac{1}{\pi}\sqrt{\frac{1}{2\Omega\pi}}\exp\left(-\frac{y^2}{4\Omega}\right)K_0\left(\frac{y^2}{4\Omega}\right). \tag{6}$$

Hereby, it should be emphasized[8] that the PDF of n_Q can be also obtained by (5).

3.2 | Binary Pulse Amplitude Modulation (BPAM)

Assuming a PLC transmitter implementing BPAM, the transmitted symbols are in $\{-A, +A\}$, where A stands for the amplitude of the transmitted symbol. The SER for BPAM can be evaluated as

$$P_e^{\text{BPAM}} = \Pr(s=A)\Pr(\tilde{s}=-A|s=A) + \Pr(s=-A)\Pr(\tilde{s}=A|s=-A). \tag{7}$$

Using (1) and using the optimal single-threshold detector with a threshold equal to 0, (7) can be rewritten as

$$\begin{aligned} P_e^{\text{BPAM}} &= \Pr(s=A)\Pr(r<0|s=A) + \Pr(s=-A)\Pr(r>0|s=-A) \\ &= \Pr(s=A)\Pr(n<-A) + \Pr(s=-A)\Pr(n>A) \end{aligned} \tag{8}$$

or, equivalently, as

$$P_e^{\text{BPAM}} = \Pr(s=A)F_{n_I}(-A) + \Pr(s=-A)\left(1-F_{n_I}(A)\right), \tag{9}$$

where $F_{n_I}(\cdot)$ represents the cumulative distribution function (CDF) of the RV n_I. We note that hereby, $n = n_I$, as BPAM is a one-dimensional modulation.

Theorem 1. *The CDF of n_I, when $m \in (0.5, 1]$, can be obtained as*

$$F_{n_I}(y) = \frac{1}{2} + \text{sgn}(y)\left[\frac{1}{2m\sqrt{\pi}}\left(\frac{my^2}{\Omega}\right)^m\frac{\Gamma(0.5-m)}{\Gamma(m)\Gamma(1-m)}\,{}_2F_2\left(m, m; m+1, m+\frac{1}{2}; -\frac{my^2}{\Omega}\right)\right.$$
$$\left. + \frac{|y|}{\pi}\sqrt{\frac{m}{\Omega}}\frac{\Gamma(m-0.5)}{\Gamma(m)}\,{}_2F_2\left(\frac{1}{2}, \frac{1}{2}; \frac{3}{2}-m, \frac{3}{2}; -\frac{my^2}{\Omega}\right)\right]. \tag{10}$$

Proof. Please refer to Appendix A. □

Theorem 2. *The CDF of n_I, when $m = 0.5$, is equal to*

$$F_{n_I}(y; m = 0.5) = \frac{1}{2} + \text{sgn}(y)\frac{1}{2\pi}\frac{|y|}{\sqrt{2\Omega}} G_{2,3}^{2,1}\left(\begin{matrix} \frac{1}{2}, \frac{1}{2} \\ 0, 0, -\frac{1}{2} \end{matrix} \middle| \frac{y^2}{2\Omega} \right). \tag{11}$$

Proof. Please refer to Appendix B. □

Substituting (10) into (9) and after some algebraic manipulations, we obtain the SER for BPAM when $m \in (0.5, 1]$ as

$$\begin{aligned} P_e^{\text{BPAM}} = \frac{1}{2} - \frac{1}{2m\sqrt{\pi}}\left(\frac{mA^2}{\Omega}\right)^m \frac{\Gamma(0.5-m)}{\Gamma(m)\Gamma(1-m)}\, {}_2F_2\left(m, m; m+\frac{1}{2}, m+1; -\frac{mA^2}{\Omega}\right) \\ - \frac{A}{\pi}\sqrt{\frac{m}{\Omega}}\frac{\Gamma(m-0.5)}{\Gamma(m)}\, {}_2F_2\left(\frac{1}{2}, \frac{1}{2}; \frac{3}{2}-m, \frac{3}{2}; -\frac{mA^2}{\Omega}\right). \end{aligned} \tag{12}$$

Meanwhile, for the special case where $m = 0.5$, we substitute (11) into (9) and get

$$P_{e,m=0.5}^{\text{BPAM}} = \frac{1}{2} - \frac{1}{2\pi}\frac{A}{\sqrt{2\Omega}} G_{2,3}^{2,1}\left(\begin{matrix} \frac{1}{2}, \frac{1}{2} \\ 0, 0, -\frac{1}{2} \end{matrix} \middle| \frac{A^2}{2\Omega} \right). \tag{13}$$

3.3 | *M*-ary Pulse Amplitude Modulation (*M*-PAM)

In this section, we generalize the results of Section 3.2, assuming M-PAM where the minimum distance between adjacent symbols is equal to $2A$. The average SER of M-PAM can be evaluated as (see chapter 5 in the work of Proakis[21])

$$P_e^{M\text{-PAM}} = \frac{2(M-1)}{M} P_e^{\text{BPAM}}. \tag{14}$$

Hence, based on (12) and (14), the average SER of M-PAM when $m \in (0.5, 1]$ is equal to

$$\begin{aligned} P_e^{M\text{-PAM}} = \frac{M-1}{M}\Bigg[1 - \frac{1}{m\sqrt{\pi}}\left(\frac{mA^2}{\Omega}\right)^m \frac{\Gamma(0.5-m)}{\Gamma(m)\Gamma(1-m)}\, {}_2F_2\left(m, m; m+\frac{1}{2}, m+1; -\frac{mA^2}{\Omega}\right) \\ - \frac{2A}{\pi}\sqrt{\frac{m}{\Omega}}\frac{\Gamma(m-0.5)}{\Gamma(m)}\, {}_2F_2\left(\frac{1}{2}, \frac{1}{2}; \frac{3}{2}-m, \frac{3}{2}; -\frac{mA^2}{\Omega}\right)\Bigg], \end{aligned} \tag{15}$$

whereas utilizing (13) and (14), when $m = 0.5$, we have

$$P_{e,m=0.5}^{M\text{-PAM}} = \frac{M-1}{M}\left[1 - \frac{A}{\pi\sqrt{2\Omega}} G_{2,3}^{2,1}\left(\begin{matrix} \frac{1}{2}, \frac{1}{2} \\ 0, 0, -\frac{1}{2} \end{matrix} \middle| \frac{A^2}{2\Omega} \right)\right]. \tag{16}$$

Hereby, after observing (15) and (16), two remarks can be made, which are validated through simulations in the following section. First of all, for given m and M values, as A^2/Ω increases, the SER decreases. In addition to this, for fixed m and A^2/Ω, increasing the modulation order M results in the increase of SER accordingly.

3.4 | Rectangular quadrature amplitude modulation

An important property of RQAM schemes is that they can be expressed as two PAM systems, ie, one in the I-axis and one in the Q-axis. To this end, we denote the PAM in the I-axis as M_I-PAM and that in the Q-axis as M_Q-PAM; hence, we have an $(M_I \times M_Q)$-ary RQAM scheme.

Proposition 1. *The average SER of PLC systems using $(M_I \times M_Q)$-RQAM and suffering from Nakagami-m background noise can be evaluated as*

$$P_e^{\text{RQAM}} = P_e^{M_I\text{-PAM}} + P_e^{M_Q\text{-PAM}} - 4\left(1 - \frac{1}{M_I}\right)\left(1 - \frac{1}{M_Q}\right)\Pr(n_I > A_I, n_Q > A_Q), \tag{17}$$

where $2A_I$ and $2A_Q$ stand for the minimum distances of the M_I-PAM and M_Q-PAM constellations, respectively.

Proof. Please refer to Appendix C. □

Observing (17), it becomes evident that in order to evaluate the SER of RQAM, we first need the CDFs of n_I and n_Q. Afterward, we should evaluate the probability of the event $\mathcal{U} = \{n_I > A_I, n_Q > A_Q\}$, which corresponds to an erroneous decision in both the M_I-PAM and the M_Q-PAM. The CDF of n_I can be derived according to Theorems 1 and 2, whereas the following lemma is used to evaluate the CDF of n_Q.

Lemma 1. *The CDF of n_Q can be obtained by (10) or (11) depending on the value of m.*

Proof. As already mentioned in Section 3.1, the PDF of n_Q is computed in the same way as that of n_I. Therefore, the CDF of n_Q can be derived following the steps in the proofs of Theorem 1 or 2 depending on the value of m. □

Next, in order to evaluate the probability of $\mathcal{U}$, it holds that

$$\Pr(n_I > A_I, n_Q > A_Q) = \int_{A_I}^{\infty}\int_{A_Q}^{\infty} f_{n_I,n_Q}(x,y)\mathrm{d}x\mathrm{d}y, \tag{18}$$

where $f_{n_I,n_Q}(x,y)$ represents the joint PDF of n_I and n_Q, which can be expressed as[22]

$$f_{n_I,n_Q}(x,y) = (x^2+y^2)^{m-1}\exp\left(-\frac{m}{\Omega}(x^2+y^2)\right). \tag{19}$$

Note that, for $m < 1$, the integral in (18) cannot be evaluated in closed form. However, it can be easily computed by using numerical integration methods.

Interestingly, for the special case where $m = 1$, utilizing equation (8.250) in the work of Gradshteyn and Ryzhik,[19] we get

$$\Pr(n_I > A_I, n_Q > A_Q; m=1) = \frac{\pi\Omega}{4}\operatorname{erfc}\left(\frac{A_I}{\sqrt{\Omega}}\right)\operatorname{erfc}\left(\frac{A_Q}{\sqrt{\Omega}}\right). \tag{20}$$

Hereby, it should be emphasized that this case, ie, $m = 1$, corresponds to the additive white Gaussian noise (AWGN) scenario.

Proposition 2. *The SER of PLC systems suffering from Nakagami-m background noise and using ($M_I \times M_Q$)-RQAM can be upper-bounded as*

$$P_{e,\mathrm{Bound}}^{\mathrm{RQAM}} = \begin{cases} P_e^{M_I\text{-PAM}} + P_e^{M_Q\text{-PAM}}, & \text{if } P_e^{M_I\text{-PAM}} + P_e^{M_Q\text{-PAM}} < 1 \\ 1, & \text{if } P_e^{M_I\text{-PAM}} + P_e^{M_Q\text{-PAM}} \geq 1. \end{cases} \tag{21}$$

Proof. Based on (17), the SER of the PLC system can be rewritten as

$$P_e^{\mathrm{RQAM}} = P_e^{M_I\text{-PAM}} + P_e^{M_Q\text{-PAM}} - \Xi(M_I, M_Q, A_I, A_Q), \tag{22}$$

where

$$\Xi(M_I, M_Q, A_I, A_Q) = 4\left(1-\frac{1}{M_I}\right)\left(1-\frac{1}{M_Q}\right)\Pr(n_I > A_I, n_Q > A_Q). \tag{23}$$

It can be observed that $\Xi(M_I, M_Q, A_I, A_Q)$ is always nonnegative, since $M_I, M_Q \geq 2$ and $\Pr(n_I > A_I, n_Q > A_Q) \in [0,1]$. As a result, we have that

$$P_e^{\mathrm{RQAM}} \leq P_e^{M_I\text{-PAM}} + P_e^{M_Q\text{-PAM}}. \tag{24}$$

Moreover, owing to the fact that P_e^{RQAM} is a probability, the following condition should be satisfied:

$$P_e^{\mathrm{RQAM}} \leq 1. \tag{25}$$

Taking into account (24) and (25), the SER of the PLC system can be upper-bounded as in (21). This concludes the proof. □

The essential difference between the bound and the actual value of SER is that the bound completely neglects the probability of the event where an erroneous decision occurs in both the M_I-PAM and M_Q-PAM systems. Therefore, as the probability of an erroneous decision in an M-PAM decreases, ie, in the high–signal-to-noise ratio (SNR) region, it is expected that the probability of a simultaneous erroneous decision in both the M_I-PAM and the M_Q-PAM becomes negligible. Therefore, in the high-SNR region, the upper bound derived by (21) can be used as a tight approximation of the ($M_I \times M_Q$)-RQAM system SER.

3.5 | Error bounds in the low-SNR regime

In order to verify the correctness of our analysis, we present well-known error bounds in the low-SNR regime. Specifically, by setting $\Omega \to \infty$ in (12), (13), (15), (16), and (24), the hypergeometric function ${}_2F_2\left(\cdot,\cdot;\cdot,\cdot;-\frac{mA^2}{\Omega}\right)$ tends to 1. Therefore, in the case of BPAM with $m \in (0.5, 1]$ and according to (12), the SER can be upper-bounded as

$$P_e^{\text{BPAM}} \leq \frac{1}{2}. \tag{26}$$

In the case of BPAM with $m = 0.5$ and since $G_{2,3}^{2,1}\left(\begin{matrix}\frac{1}{2},\frac{1}{2}\\ 0,0,-\frac{1}{2}\end{matrix}\middle| 0\right) = 0$, the SER can also be upper-bounded as

$$P_{e,m=0.5}^{\text{BPAM}} \leq \frac{1}{2}. \tag{27}$$

In the case of M-PAM with a low SNR, by using (26) and (27), the SER is bounded by

$$P_e^{\text{MPAM}} \leq \frac{M-1}{M}. \tag{28}$$

Similarly, in the case of RQAM, in the low-SNR regime, the SER can be bounded as

$$P_e^{\text{RQAM}} \leq \min\left(\frac{M_I-1}{M_I} + \frac{M_Q-1}{M_Q}, 1\right), \tag{29}$$

where $\min(\cdot,\cdot)$ denotes the minimum operator. Note that these expressions are considered trivial for the AWGN scenario, but they are not obvious in this case.

4 | RESULTS AND DISCUSSION

In this section, the effect of Nakagami-m noise on the error performance of the PLC system is investigated by illustrating analytical and Monte Carlo simulation results for different modulation schemes and realistic noise parameters. In particular, we assume that $10^7 \log_2 M$ data bits are transmitted in order to evaluate the average SER, where M stands for the modulation order. The SNR is denoted as $\mathcal{E}_s/\Omega$, with $\mathcal{E}_s$ representing the average symbol energy, which can be expressed as

$$\mathcal{E}_s^{M\text{-PAM}} = \frac{M^2-1}{3}A^2, \tag{30}$$

for M-PAM, whereas it is equal to

$$\mathcal{E}_s^{\text{RQAM}} = \frac{M_I^2-1}{3}A_I^2 + \frac{M_Q^2-1}{3}A_Q^2, \tag{31}$$

in the case of $(M_I \times M_Q)$-RQAM.

Figure 1 depicts the SER with respect to SNR, for different values of m, assuming BPAM. Firstly, it becomes evident that the analytical results are identical to the simulation ones, and thus, the presented mathematical framework is verified. Additionally, as expected, the SER decreases with the increase in SNR. Besides, the error performance of the PLC system improves with the increase in m for a specific SNR value, especially in the high-SNR region. This is rational and can be explained by the fact that as m approaches 1, the distribution of the background noise amplitude approaches the Rayleigh one.[4] Consequently, the real part of the background noise tends to reduce to AWGN, which has been proven to be the noise type resulting in the best error performance of a communication system.

In Figure 2, the average SER versus SNR, for different values of m and M-PAM schemes, is illustrated. This Figure validates the accuracy of (15) and (16). Moreover, we observe that, for given SNR and m, as the modulation order increases, the reliability of the PLC system decreases. Besides, for higher M values, the increase in m results in a lower enhancement of the SER.

Next, we present the impact of Nakagami-m background noise on the error performance of PLC systems that use $(M_I \times M_Q)$-RQAM. Specifically, in Figure 3, the SER of (2×2)-RQAM and (2×4)-RQAM is demonstrated with respect to the SNR for different values of m. The upper bound of the SER derived in (21) is also illustrated. We observe that the analytical results are in accordance with the Monte Carlo simulation results, whereas in the high-SNR region, the upper bound is very tight. This indicates that the derived closed-form expression of the SER upper bound can be used as a key error performance indicator, when designing PLC systems.

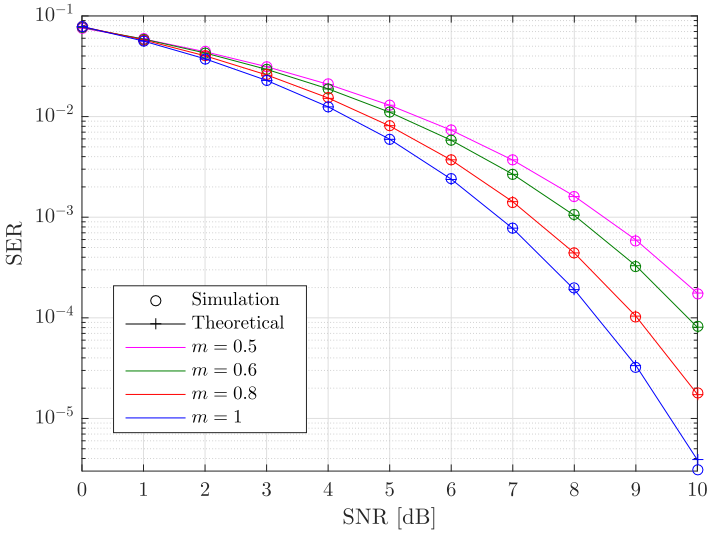

FIGURE 1 Average SER versus SNR employing BPAM

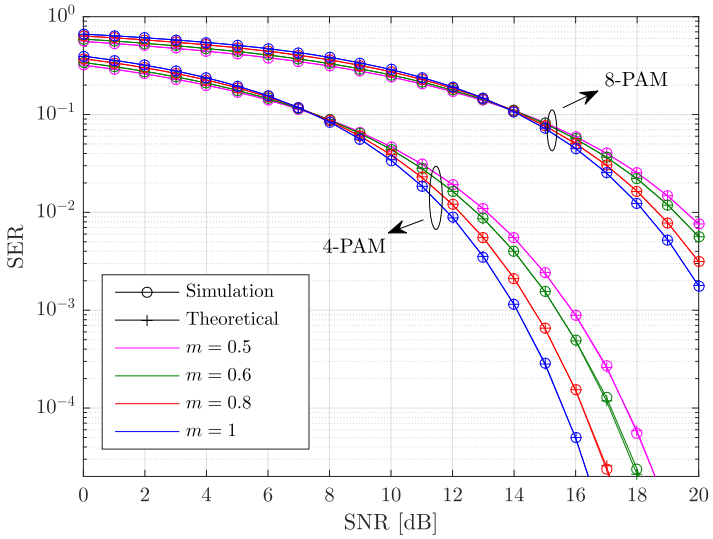

FIGURE 2 Average SER versus SNR employing 4-PAM or 8-PAM

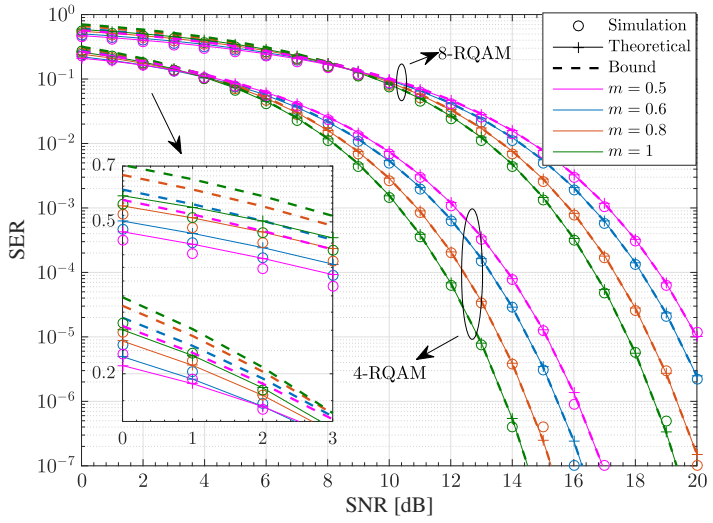

FIGURE 3 Average SER versus SNR employing 4-RQAM or 8-RQAM

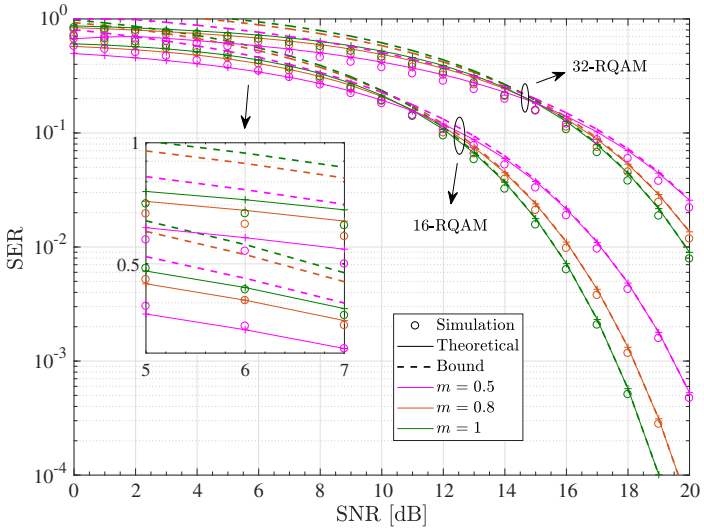

FIGURE 4 SER versus SNR employing 16-RQAM or 32-RQAM

Similarly, Figure 4 illustrates the average SER of PLC systems for different values of m, assuming (4×4)-RQAM or (4×8)-RQAM. As expected, for fixed M and m values, an increase in the SNR results in an SER decrease. Moreover, for the same m and SNR value, an increase in M has a detrimental effect on the system error rate performance.

Finally, a very interesting remark concerns the error performance in the lower-SNR region. More precisely, it is observed that in the low-SNR regime, the error performance is enhanced as m decreases. This is more evident in the RQAM schemes. This is a very interesting result, which is due to the nature of the Nakagami-m distribution. More specifically, with a change in the m parameter—also known as the shape parameter—the shape of the noise distribution varies, and in the low-SNR regime, a system with lower m performs better. However, in higher SNRs, the performance improves with m. This can be easily concluded if someone plots the Nakagami-m PDF for several values of m.

5 | CONCLUSION

In this paper, the error performance of PLC systems under additive background noise with Nakagami-m distributed magnitude and uniformly distributed phase has been investigated, assuming different modulation schemes. In more detail, we have derived novel closed-form expressions for the SER of M-PAM schemes and used them to evaluate the SER assuming $(M_I \times M_Q)$-RQAM. In addition, a novel upper bound for the error probability of PLC systems that use RQAM has been presented. The derived SER upper bound can be used as a key error performance indicator, when designing PLC systems. Finally, our findings revealed the importance of considering the impact of Nakagami-m background noise, during the design and deployment of PLC systems.

ACKNOWLEDGEMENT

The work of G. D. Ntouni has been supported by a scholarship from the Alexander Onassis Foundation.

ORCID

George K. Karagiannidis http://orcid.org/0000-0001-8810-0345

REFERENCES

1. Majumder A, Caffery J. Power line communications. *IEEE Potentials*. 2004;23(4):4-8.
2. Goel S, Bush SF, Bakken D. *IEEE Vision for Smart Grid Communications: 2030 and Beyond Roadmap*. Piscataway, NJ: IEEE Communications Society; 2013.
3. Latchman HA, Katar S, Yonge L, Gavette S. *Homeplug AV and IEEE 1901: A Handbook for PLC Designers and Users*. Hoboken, NJ: John Wiley & Sons; 2013.

4. Meng H, Guan YL, Chen S. Modeling and analysis of noise effects on broadband power-line communications. *IEEE Trans Power Del*. 2005;20(2):630-637.
5. Tao Z, Xiaoxian Y, Baohui Z, Xu NH, Xiaoqun F, Changxin L. Statistical analysis and modeling of noise on 10-kV medium-voltage power lines. *IEEE Trans Power Del*. 2007;22(3):1433-1439.
6. Kim Y, Choi S, Oh HM. Closed-form expression of Nakagami-like background noise in power-line channel. *IEEE Trans Power Del*. 2008;23(3):1410-1412.
7. Kim Y, Oh HM, Choi S. BER performance of binary transmitted signal for power line communication under Nakagami-like background noise. Paper presented at: The First International Conference on Smart Grids, Green Communications and IT Energy-Aware Technologies; 2011; Venice, Italy.
8. Kim Y, Rhee SW, Lee JJ, Oh SK. BER performance of QPSK-transmitted signal for power line communication under Nakagami-like background noise. *J Int Counc Electr Eng*. 2014;4(1):54-58.
9. Chattopadhyay A, Sharma K, Chandra A. Error performance of RS coded binary FSK in PLC channels with Nakagami and impulsive noise. Paper presented at: 18th IEEE International Symposium on Power Line Communications and Its Applications; 2014; Glasgow, UK.
10. Mathur A, Bhatnagar MR. PLC performance analysis assuming BPSK modulation over Nakagami-*m* additive noise. *IEEE Commun Lett*. 2014;18(6):909-912.
11. Mathur A, Bhatnagar MR, Panigrahi BK. Maximum likelihood decoding of QPSK signal in power line communications over Nakagami-m additive noise. Paper presented at: 2015 IEEE International Symposium on Power Line Communications and Its Applications (ISPLC); 2015; Austin, TX.
12. Mathur A, Bhatnagar MR, Panigrahi BK. Outage probability analysis of PLC with channel gain under Nakagami-m additive noise. Paper presented at: 2015 IEEE 82nd Vehicular Technology Conference (VTC2015-Fall); 2015; Boston, MA.
13. Mathur A, Bhatnagar MR, Panigrahi BK. On the performance of a PLC system assuming differential binary phase shift keying. *IEEE Commun Lett*. 2016;20(4):668-671.
14. Chandra A, Gupta A, Mallick D, Mishra AK. Performance of BFSK over a PLC channel corrupted with background Nakagami noise. Paper presented at: 2010 IEEE International Conference on Communication Systems; 2010; Singapore.
15. Ndo G, Siohan P, Hamon MH. Adaptive noise mitigation in impulsive environment: application to power-line communications. *IEEE Trans Power Del*. 2010;25(2):647-656.
16. Agrawal N, Sharma PK. Capacity analysis of a NBPLC system with background and impulsive noises. Paper presented at: 2017 International Conference on Computer, Communications and Electronics (Comptelix); 2017; Jaipur, India.
17. Dash SP, Mallik RK, Mohammed SK. Coherent detection in a receive diversity PLC system under Nakagami-m noise environment. Paper presented at: 2016 IEEE 27th Annual International Symposium on Personal, Indoor, and Mobile Radio Communications (PIMRC); 2016; Valencia, Spain.
18. Juwono FH, Guo Q, Chen Y, Xu L, Huang DD, Wong KP. Linear combining of nonlinear preprocessors for OFDM-based power-line communications. *IEEE Trans Smart Grid*. 2016;7(1):253-260.
19. Gradshteyn IS, Ryzhik IM. *Table of Integrals, Series, and Products*. 6th ed. New York, NY: Academic Press; 2000.
20. Prudnikov AP, Brychkov YA, Marichev OI. *Special Functions*. Amsterdam, The Netherlands: Gordon and Breach Science Publishers; 1986. *Integrals and Series*; vol. 2.
21. Proakis JG. *Digital Communications*. New York, NY: McGraw-Hill; 2001. *Electrical Engineering Series*.
22. Fraidenraich G, Leveque O, Cioffi JM. On the MIMO channel capacity for the Nakagami-*m* channel. *IEEE Trans Inf Theory*. 2008;54(8):3752-3757.
23. Papoulis A, Pillai SU. *Probability, Random Variables, and Stochastic Processes*. New York, NY: McGraw-Hill; 2002. *McGraw-Hill Series in Electrical Engineering: Communications and Signal Processing*.

How to cite this article: Papanikolaou VK, Ntouni GD, Boulogeorgos A-AA, Karagiannidis GK. Error performance of power line communications in the presence of Nakagami-*m* background noise. *Trans Emerging Tel Tech*. 2018;29:e3475. https://doi.org/10.1002/ett.3475

APPENDIX A

PROOF OF THEOREM 1

Assuming $m \in (0.5, 1]$, the CDF of the RV n_I can be evaluated as

$$F_{n_I}(x) = \int_{-\infty}^{x} f_{n_I}(y)\mathrm{d}y, \tag{A1}$$

where $f_{n_I}(y)$ is given by (5). Since $f_{n_I}(y)$ is symmetric around 0, (A1) can be rewritten as

$$F_{n_I}(x) = \begin{cases} \frac{1}{2} + \int_0^x f_{n_I}(y)\mathrm{d}y, & x \geq 0 \\ \frac{1}{2} - \int_{-x}^0 f_{n_I}(y)\mathrm{d}y, & x < 0 \end{cases} \tag{A2}$$

or, equivalently,

$$F_{n_I}(x) = \begin{cases} \frac{1}{2} + \int_0^x f_{n_I}(y)\mathrm{d}y, & x \geq 0 \\ \frac{1}{2} - \int_0^{|x|} f_{n_I}(y)\mathrm{d}y, & x < 0. \end{cases} \tag{A3}$$

By combining the two branches of (A3), we can easily express the CDF of n_I, $F_{n_I}(x)$, as

$$F_{n_I}(x) = \frac{1}{2} + \mathrm{sgn}(x)\mathcal{I}(x), \tag{A4}$$

where

$$\mathcal{I}(x) = \int_0^{|x|} f_{n_I}(y)\mathrm{d}y. \tag{A5}$$

Substituting (5) into (A5) and after some algebraic manipulations, (A5) can be written as

$$\mathcal{I}(x) = B(x) + C(x), \tag{A6}$$

where

$$B(x) = \frac{1}{\sqrt{\pi}}\sqrt{\frac{m}{\Omega}}\,\frac{\Gamma(0.5-m)}{\Gamma(m)\Gamma(1-m)}\int_0^{|x|}\left(\frac{my^2}{\Omega}\right)^{m-\frac{1}{2}}\exp\left(-\frac{my^2}{\Omega}\right){}_1F_1\left(\frac{1}{2},\frac{1}{2}+m,\frac{my^2}{\Omega}\right)\mathrm{d}y \tag{A7}$$

and

$$C(x) = \frac{\Gamma(m-0.5)}{\pi\Gamma(m)}\sqrt{\frac{m}{\Omega}}\int_0^{|x|}\exp\left(-\frac{my^2}{\Omega}\right){}_1F_1\left(1-m,\frac{3}{2}-m,\frac{my^2}{\Omega}\right)\mathrm{d}y. \tag{A8}$$

Afterward, by setting $z = \frac{m}{\Omega}y^2$ into (A7) and (A8), we respectively obtain

$$B(x) = \frac{1}{2\sqrt{\pi}}\,\frac{\Gamma(0.5-m)}{\Gamma(m)\Gamma(1-m)}\int_0^{\frac{m}{\Omega}x^2}{}_1F_1\left(\frac{1}{2},\frac{1}{2}+m,z\right)z^{m-1}\exp(-z)\,\mathrm{d}z \tag{A9}$$

and

$$C(x) = \frac{\Gamma(m-0.5)}{2\pi\Gamma(m)}\int_0^{\frac{m}{\Omega}x^2}{}_1F_1\left(1-m,\frac{3}{2}-m,z\right)z^{-\frac{1}{2}}\exp(-z)\,\mathrm{d}z. \tag{A10}$$

Next, using equation (1.14.1.8) in the work of Prudnikov et al,[20] ie,

$$\int_0^x z^{a-1}\exp(-bz)\,{}_1F_1(c,d,bz)\mathrm{d}z = \frac{x^a}{a}\,{}_2F_2(a,d-c;d,a+1;-bx), \tag{A11}$$

we get closed-form expressions for (A9) and (A10) as

$$B(x) = \frac{1}{2m\sqrt{\pi}}\left(\frac{mx^2}{\Omega}\right)^m\frac{\Gamma(0.5-m)}{\Gamma(m)\Gamma(1-m)}\,{}_2F_2\left(m,m;m+\frac{1}{2},m+1;-\frac{mx^2}{\Omega}\right) \tag{A12}$$

and

$$C(x) = \frac{|x|}{\pi}\sqrt{\frac{m}{\Omega}}\frac{\Gamma(m-0.5)}{\Gamma(m)}\,{}_2F_2\left(\frac{1}{2},\frac{1}{2};\frac{3}{2}-m,\frac{3}{2};-\frac{mx^2}{\Omega}\right). \tag{A13}$$

Substituting (A12) and (A13) in (A6), we have

$$\mathcal{I}(x) = \frac{1}{2m\sqrt{\pi}} \left(\frac{mx^2}{\Omega}\right)^m \frac{\Gamma(0.5-m)}{\Gamma(m)\Gamma(1-m)} \times {}_2F_2\left(m, m; m+\frac{1}{2}, m+1; -\frac{mx^2}{\Omega}\right) + \frac{|x|}{\pi}\sqrt{\frac{m}{\Omega}} \frac{\Gamma(m-0.5)}{\Gamma(m)} {}_2F_2\left(\frac{1}{2}, \frac{1}{2}; \frac{3}{2}-m, \frac{3}{2}; -\frac{mx^2}{\Omega}\right). \tag{A14}$$

Finally, combining (A14) and (A4), we derive (10). This completes the proof.

APPENDIX B

PROOF OF THEOREM 2

Assuming $m = 0.5$, the CDF of n_I can be obtained similarly to the $m \in (0.5, 1]$ case in Appendix A, ie,

$$F_{n_I}(x; m = 0.5) = \frac{1}{2} + \text{sgn}(x)\mathcal{J}(x), \tag{B1}$$

where

$$\mathcal{J}(x) = \int_0^{|x|} f_{n_I}(y; m = 0.5)\mathrm{d}y. \tag{B2}$$

Substituting (6) into (B2), we get

$$\mathcal{J}(x) = \frac{1}{\pi}\sqrt{\frac{1}{2\Omega\pi}} \int_0^{|x|} \exp\left(-\frac{y^2}{4\Omega}\right) K_0\left(\frac{y^2}{4\Omega}\right) \mathrm{d}y, \tag{B3}$$

which, after setting $t = \frac{y^2}{4\Omega}$, can be rewritten as

$$\mathcal{J}(x) = \frac{1}{\pi}\sqrt{\frac{1}{2\pi}} \int_0^{\frac{x^2}{4\Omega}} t^{-1/2} \exp(-t) K_0(t) \mathrm{d}t. \tag{B4}$$

Now, using equation (9.304/4) in the work of Gradshteyn and Ryzhik,[19] (B2) can be expressed as

$$\mathcal{J}(x) = \frac{1}{\pi\sqrt{2}} \int_0^{\frac{x^2}{4\Omega}} t^{-1/2} G_{1,2}^{2,0}\left(\begin{matrix}\frac{1}{2} \\ 0, 0\end{matrix}\middle| 2t\right) \mathrm{d}t, \tag{B5}$$

whereas using equation (2.24.2/2) in the work of Prudnikov et al,[20] we have

$$\mathcal{J}(x) = \frac{1}{2\pi} \frac{|x|}{\sqrt{2\Omega}} G_{2,3}^{2,1}\left(\begin{matrix}\frac{1}{2}, \frac{1}{2} \\ 0, 0, -\frac{1}{2}\end{matrix}\middle| \frac{x^2}{2\Omega}\right). \tag{B6}$$

Finally, substituting (B6) into (B1), we derive (11). This concludes the proof.

APPENDIX C

PROOF OF PROPOSITION 1

In order to enhance the readability of the proof, we first denote the following events.

- $\mathcal{B}_I$: Erroneous decision in the M_I-PAM
- $\mathcal{B}_Q$: Erroneous decision in the M_Q-PAM
- $\mathcal{B}_{I\cup Q}$: Erroneous decision in the M_I-PAM and/or the M_Q-PAM
- $\mathcal{B}_{I\cap Q}$: Erroneous decision in both the M_I-PAM and the M_Q-PAM

Thus, the average SER is equal to[23]

$$P_e^{\text{RQAM}} = \Pr(\mathcal{B}_{I\cup Q}) = \Pr(\mathcal{B}_I) + \Pr(\mathcal{B}_Q) - \Pr(\mathcal{B}_{I\cap Q}). \tag{C1}$$

From Bayes' Theorem, it holds that

$$\Pr(\mathcal{B}_{I\cap Q}) = \Pr(\mathcal{B}_Q)\Pr(\mathcal{B}_I|\mathcal{B}_Q). \tag{C2}$$

Now, following the analysis that is commonly utilized in the literature in order to derive the probability of an erroneous decision in a PAM scheme,[21] we get

$$\Pr(\mathcal{B}_I|\mathcal{B}_Q) = 2\left(1-\frac{1}{M_I}\right)\Pr(n_I > A_I|\mathcal{B}_Q), \tag{C3}$$

and using Bayes' theorem, (C3) becomes

$$\Pr(\mathcal{B}_I|\mathcal{B}_Q) = 2\left(1-\frac{1}{M_I}\right)\Pr(\mathcal{B}_Q|n_I > A_I)\frac{\Pr(n_I > A_I)}{\Pr(\mathcal{B}_Q)}. \tag{C4}$$

Afterward, utilizing (C3), $\Pr(\mathcal{B}_Q|n_I > A_I)$ is equal to

$$\Pr(\mathcal{B}_Q|n_I > A_I) = 2\left(1-\frac{1}{M_Q}\right)\Pr(n_Q > A_Q|n_I > A_I). \tag{C5}$$

Substituting (C5) into (C4), we have

$$\Pr(\mathcal{B}_I|\mathcal{B}_Q) = 4\left(1-\frac{1}{M_I}\right)\left(1-\frac{1}{M_Q}\right)\Pr(n_Q > A_Q|n_I > A_I)\frac{\Pr(n_I > A_I)}{\Pr(\mathcal{B}_Q)}. \tag{C6}$$

Taking into account Bayes' theorem, it holds that

$$\Pr(\mathcal{B}_I|\mathcal{B}_Q) = 4\left(1-\frac{1}{M_I}\right)\left(1-\frac{1}{M_Q}\right)\frac{\Pr(n_Q > A_Q \cap n_I > A_I)}{\Pr(\mathcal{B}_Q)}. \tag{C7}$$

Hereby, substituting (C7) into (C2) and taking into account that

$$\Pr(\mathcal{U}) = \Pr(n_I > A_I, n_Q > A_Q) = \Pr(n_I > A_I \cap n_Q > A_Q), \tag{C8}$$

we obtain

$$\Pr(\mathcal{B}_{I\cap Q}) = 4\left(1-\frac{1}{M_I}\right)\left(1-\frac{1}{M_Q}\right)\Pr(n_I > A_I, n_Q > A_Q). \tag{C9}$$

Finally, substituting (C9) into (C1), we derive (17). This concludes the proof.